



Black hole to grey hole metamorphosis in the deep quantum regime

Harpreet Singh^a, Malay K. Nandy^b 

Department of Physics, Indian Institute of Technology Guwahati, Guwahati 781 039, India

Received: 7 September 2024 / Accepted: 20 November 2024
© The Author(s) 2024

Abstract In order to search for new solutions for collapsed objects in quantum gravity, we consider in this paper a Kantowski–Sachs metric labelled by parameters that have no classical significance. In addition, we include a Klein–Gordon field to represent in a simple manner the inevitable zero-point vacuum fluctuations that permeate the spacetime. With this framework, we quantize the system and obtain the Wheeler–DeWitt equation in order to focus upon the deep quantum regime of the interior and to analyze any kind of transition that the black hole may undergo. The Wheeler–DeWitt equation reveals the existence of new solutions of different nature, designated herein as “quantum grey holes,” in addition to the existence of quantum black holes, with all solutions satisfying the DeWitt boundary condition. The existence of new solutions gives rise to the novel possibility of a quantum black hole making a transition to a quantum grey hole. We find that there exists non-zero probability of quantum black-to-grey hole transition. These transition probabilities exhibit resonances for a continuous range of eigenvalues of the system.

1 Introduction

The mysteries of black hole evaporation as shown by Hawking [1,2], as well as the singularity [3–6] in its interior, are some of the biggest challenges of theoretical physics. However, the phenomenon of black hole evaporation still does not have a complete picture. At the end of black hole evaporation, there should be a smooth spacetime for the validity of well-known physical laws [7].

General relativity fails to provide an explanation for the spacetime at the central singularity of the black hole. The

first classical attempt to obtain a regular spacetime at the center was made by Bardeen [8] by replacing the mass of the black hole with a space-dependent function. Hayward [9] constructed a regular black hole by including a length scale in the metric. He showed that such a regular black hole has trapped surfaces having inner and outer boundaries, with the inner boundary never reaching any singularity. He [10] further argued that such regular black holes evaporate completely without having to hit any singularity.

However, one expects that a regular black hole without any singularity should follow in a more natural way, for example, by quantum mechanical treatment of the spacetime. In quantum theories of gravity, such as string theory [11, 12] and loop quantum gravity [13–15], black hole singularity resolution follows naturally. It is also important to have a regular spacetime at the end of black hole evaporation. Various ways of singularity resolution are discussed in Refs. [16–21].

However, even in quantum gravity scenarios, the behavior of collapsing matter near the singularity is not well-understood yet. Smolin [22] argued that the collapsing matter may emerge into a baby universe by cosmological natural selection.

Frolov and Vilkovisky [23] considered spherical collapse of a null shell in an effective theory of gravity with quantum effects at one loop order. They showed that the shell collapses to $r = 0$ without the appearance of any singularity and it starts expanding thereafter.

Hájček and Kiefer [24–26] showed that an in-falling null spherical shell can expand due to a bounce. Ambrus and Hájček [27] estimated the bouncing time by introducing a spherical mirror in the system and showed that it is in the order of twice the time light would take to travel between the mirror and observer in flat spacetime.

Ashketar et al. [28, 29] resolved the big bang singularity in the Friedman model by showing that the wave function

^a e-mail: harpreetsingh@iitg.ac.in

^b e-mail: mknandy@iitg.ac.in (corresponding author)

of the collapsing universe tunnels into an expanding one, so that the big bang singularity is replaced by a big bounce.

Haggard and Rovelli [30] showed that there exists a classical metric, excluding a finite region around the singularity, satisfying the Einstein field equation, with the possibility of a black hole bouncing into a white hole. They argued that the black hole can tunnel into a white hole due to accumulation of quantum gravity effects over a sufficiently long time.

Lorenzo and Perez [31] carried out a semiclassical stability analysis of the above bouncing black hole model [30] against quantum fluctuations in the energy–momentum tensor. They found that the model is highly unstable due to a long lived trapping horizon in the white hole phase. To resolve the issue of instability, they proposed a time asymmetric version of the model with a slow black hole phase followed by a fast white hole phase.

Han et al. [32] considered the Oppenheimer–Snyder model of a collapsing star with quantum correction to the spherically symmetric metric. The resulting Reissner–Nordström-like geometry facilitates interpolation between black hole and white hole horizons giving a bouncing dynamics. Interestingly, Rignon-Bret and Rovelli [33] had earlier shown that a Reissner–Nordström black hole can also tunnel to a white hole.

Frisoni [34], in the framework of loop quantum gravity, calculated the black hole to white hole transition amplitude numerically in the spinfoam formulation. This facilitated obtaining estimates for the transition amplitude in the deep quantum regime.

We thus see that it is important to focus upon the deep quantum regime of the black hole interior in order to analyze any kind of transition that the black hole may undergo. We therefore consider the quantum nature of the black hole interior predicted by quantum gravity and analyze the transitions in terms of the wave function of the interior geometry.

We achieve this goal by solving the Wheeler–DeWitt equation [35, 36] in the black hole interior with a special form of the Kantowski–Sachs metric [37] labelled by parameters defining different regions of the parameter space. We ensure resolution of the classical singularity so that the interior wave function satisfies the DeWitt boundary condition [36]. In obtaining the analytical solutions of the Wheeler–DeWitt equation, we adopt a procedure similar to Ref. [38] where the Hilbert space was shown to have three non-overlapping sectors depending on the relative magnitudes of the eigenvalues. In this work, we neglect the unphysical sector and consider the remaining two sectors for the discussion of quantum transitions of the black hole.

We find that there exist new solutions for the interior wave function in three different regions of the parameter space which satisfy the DeWitt boundary condition. Since these solutions have a different nature than the black hole wave function, we designate them as “quantum grey holes.” Fur-

thermore, we find that there exists non-zero probability of transition from the quantum black hole state to the quantum grey hole state. These transition probabilities also exhibit resonances for a continuous range of eigenvalues of the system. We illustrate the transition probabilities with various plots in different perspectives of the eigenvalues. We illustrate the transition probabilities with various plots in different perspectives of the eigenvalues.

We organise the rest of the paper in the following way. In Sect. 2, we present the model of Kantowski–Sachs metric labelled by parameters which will play a significant role in determining the solution of the Wheeler–DeWitt equation. In Sect. 3, we obtain the Hamiltonian of the gravitational part that follows from the Kantowski–Sachs metric. In addition, we include the Hamiltonian of a Klein–Gordon field as a simple representation of spontaneous zero-point vacuum fluctuations, that inevitably permeates the spacetime of the hole. We quantize the system in Sect. 4 and obtain the Wheeler–DeWitt equation of the system. We also solve the Wheeler–DeWitt equation in Sect. 4 employing standard methods for partial differential equations and obtain a general form of the wave function. Depending on the sign parameters coming from the metric, we characterize the solutions into quantum black/grey holes. In Sects. 5 and 6, we calculate the probability of a black hole making a transition to a grey hole. We also illustrate in Sects. 5 and 6 the black-to-grey hole transition probabilities with various plots in different perspectives of the eigenvalues. Finally, in Sect. 7, we present a discussion and conclusion.

2 Kantowski–Sachs model

We represent the black hole interior spacetime with a Kantowski–Sachs metric [37], having the form

$$ds^2 = -\{c\alpha(t)\}^2 dt^2 + \{a\xi(t)\}^2 dr^2 + \{b\zeta(t)\}^2 d\Omega^2, \quad (1)$$

where $d\Omega^2 = d\theta^2 + \sin^2\theta d\varphi^2$, and the parameters a , b and c can each take the values ± 1 .

Classically, the above metric (1) is exactly equivalent to $ds^2 = -\alpha^2(t)dt^2 + \xi^2(t)dr^2 + \zeta^2(t)d\Omega^2$. However, quantum mechanically, the sign parameters a and b will make a substantial difference in the picture, as they appear in the expression of the interior wave function, which depends on the square root of the spatial metric coefficients.

Quantum black hole solutions are obtained for $a = b = +1$, as discussed in Ref. [38]. In the remaining three quadrants, with other signs of the parameters a and b , the wave functions differ from the black hole solutions, called herein “quantum grey hole” solutions.

Since the wave functions are distinct in nature, we study transition of the quantum black hole to a quantum grey hole.

We compute the transition probabilities in the two physical sectors and find that there are non-zero probabilities of making the transition. The probability of transition depends strongly on the eigenvalues and, interestingly, these exist resonances at specific eigenvalues.

3 System Hamiltonian

In this section, we shall construct the classical Hamiltonian of the system described by the Kantowski–Sachs metric (1).

The gravitational part of the Lagrangian is given by

$$L_g = \int \frac{1}{16\pi G} \sqrt{-g} \left(K_{ij} K^{ij} - K^2 + {}^{(3)}R \right) d^3x, \tag{2}$$

With the metric (1), the spatial curvature ${}^{(3)}R$ and extrinsic curvature K_{ij} are obtained as

$${}^{(3)}R = \frac{2}{\{b\dot{\zeta}(t)\}^2} \tag{3}$$

and

$$K_{ij} = -(c\alpha)^{-1} \text{diag} \left(a^2 \xi \dot{\xi}, b^2 \zeta \dot{\zeta}, b^2 \zeta \dot{\zeta} \sin^2 \theta \right). \tag{4}$$

Thus the Lagrangian (2) takes the form

$$L_g = \frac{r_0}{4G} \frac{(a\xi)(b\zeta)^2}{(c\alpha)} \left[-4 \frac{\dot{\xi}\dot{\zeta}}{\xi\zeta} - 2 \frac{\dot{\zeta}^2}{\zeta^2} + \frac{2}{(b\zeta)^2} c^2 \alpha^2 \right], \tag{5}$$

where $r_0 = \int dr$ is a fiducial parameter.

The canonical momenta conjugate to ξ and ζ can therefore be calculated as

$$P_\xi = \frac{\partial L_g}{\partial \dot{\xi}} = -\frac{r_0}{4G} \frac{1}{(c\alpha)} (a\xi)(b\zeta)^2 \frac{4\dot{\zeta}}{\xi\zeta} \tag{6}$$

and

$$P_\zeta = \frac{\partial L_g}{\partial \dot{\zeta}} = -\frac{r_0}{4G} \frac{1}{(c\alpha)} (a\xi)(b\zeta)^2 \left(4 \frac{\dot{\zeta}}{\zeta^2} + 4 \frac{\dot{\xi}}{\xi\zeta} \right), \tag{7}$$

Thus the gravitational Hamiltonian $H_g = P_\xi \dot{\xi} + P_\zeta \dot{\zeta} - L_g$ is obtained as

$$H_g = \frac{4Gc\alpha}{r_0 a \xi b^2 \zeta^2} \left(-\frac{\xi\zeta P_\xi P_\zeta}{4} + \frac{1}{8} (\xi P_\xi)^2 - \frac{r_0^2}{8G^2} a^2 b^2 \xi^2 \zeta^2 \right). \tag{8}$$

Since we shall formulate a quantum theory, spontaneous vacuum fluctuations of matter fields have to be accounted

for. We shall take a massless Klein–Gordon field as a simple representation of the matter fields, with Lagrangian

$$L_\phi = - \int \frac{1}{2} \sqrt{-g} g^{\mu\nu} \partial_\mu \phi \partial_\nu \phi d^3x. \tag{9}$$

In our simple representation of the interior geometry by the Kantowski–Sachs metric (1), the metric coefficients depend only on the time. In a similar manner, we shall take the Klein–Gordon field to be only time dependent, leading to

$$L_\phi = \frac{2\pi r_0}{c\alpha} a \xi b^2 \zeta^2 \dot{\phi}^2. \tag{10}$$

Thus the canonical momentum is

$$P_\phi = \frac{\partial L_\phi}{\partial \dot{\phi}} = \frac{4\pi r_0}{c\alpha} a \xi b^2 \zeta^2 \dot{\phi}, \tag{11}$$

giving the Klein–Gordon Hamiltonian as

$$H_\phi = P_\phi \dot{\phi} - L_\phi = \frac{c\alpha}{8\pi r_0} \frac{P_\phi^2}{a \xi b^2 \zeta^2}. \tag{12}$$

The total Hamiltonian $H = H_g + H_\phi$ is therefore given by

$$H = \frac{c\alpha G}{r_0 a \xi b^2 \zeta^2} \left(-\xi\zeta P_\xi P_\zeta + \frac{1}{2} (\xi P_\xi)^2 - \frac{r_0^2}{2G^2} a^2 \xi^2 b^2 \zeta^2 + \frac{P_\phi^2}{8\pi G} \right). \tag{13}$$

In the next section, we shall quantize this Hamiltonian (13) following standard prescriptions of quantum mechanics to obtain the Wheeler–DeWitt equation.

4 Wheeler–DeWitt wave function

In order to quantize the system, we promote the canonical momenta to operators with the prescriptions: $P_\xi \rightarrow -i\hbar \frac{\partial}{\partial \xi}$, $P_\zeta \rightarrow -i\hbar \frac{\partial}{\partial \zeta}$ and $P_\phi \rightarrow -i\hbar \frac{\partial}{\partial \phi}$. Consequently, the Hamiltonian (13) is also promoted to an operator $H \rightarrow \hat{H}$, giving the Wheeler–DeWitt equation $\hat{H} \Psi = 0$ in the form

$$\left(\xi\zeta \frac{\partial^2}{\partial \xi \partial \zeta} - \frac{\xi^2}{2} \frac{\partial^2}{\partial \xi^2} - \frac{\xi}{2} \frac{\partial}{\partial \xi} - \frac{r_0^2}{2\hbar^2 G^2} a^2 \xi^2 b^2 \zeta^2 - \frac{1}{8\pi G} \frac{\partial^2}{\partial \phi^2} \right) \Psi = 0, \tag{14}$$

The Hamiltonian does not depend on ϕ explicitly and the Wheeler–DeWitt equation is separable in ϕ . Writing

$\Psi(\xi, \zeta, \phi) = \psi(\xi, \zeta)e^{-i\kappa\phi}$ reduces equation (14) to

$$\left(\xi\zeta \frac{\partial^2}{\partial \xi \partial \zeta} - \frac{\xi^2}{2} \frac{\partial^2}{\partial \xi^2} - \frac{\zeta}{2} \frac{\partial}{\partial \xi} - \frac{r_0^2}{2\hbar^2 G^2} a^2 \xi^2 b^2 \zeta^2 + \frac{\kappa^2}{8\pi G} \right) \psi = 0, \tag{15}$$

To solve Eq. (15), we transform the variables as

$$z = a\xi b\zeta \quad \text{and} \quad x = a\xi, \tag{16}$$

so that Eq. (15) is transformed to

$$\left(z^2 \frac{\partial^2}{\partial z^2} + z \frac{\partial}{\partial z} - x^2 \frac{\partial^2}{\partial x^2} - x \frac{\partial}{\partial x} - \frac{r_0^2}{\hbar^2 G^2} z^2 + \frac{\kappa^2}{4\pi G} \right) \psi = 0. \tag{17}$$

Substituting $\psi(z, x) = Z(z)X(x)$ in (17), we get two ordinary differential equations,

$$z^2 \frac{\partial^2 Z}{\partial z^2} + z \frac{\partial Z}{\partial z} - \frac{r_0^2}{\hbar^2 G^2} z^2 Z - \lambda Z = 0 \tag{18}$$

and

$$x^2 \frac{\partial^2 X}{\partial x^2} + x \frac{\partial X}{\partial x} - \frac{\kappa^2}{4\pi G} X - \lambda X = 0. \tag{19}$$

Equation (18) is Bessel differential equation whose solution is

$$Z(z) = c_1 J_\nu(i\tilde{z}) + c_2 Y_\nu(i\tilde{z}), \tag{20}$$

where $J_\nu(i\tilde{z})$ and $Y_\nu(i\tilde{z})$ are respectively the Bessel functions of first and second kind of order $\nu = \sqrt{\lambda}$, and $\tilde{z} = \frac{r_0}{\hbar G} z$, with c_1 and c_2 arbitrary constants.

Equation (19) admits power law type solutions of the form

$$X(x) = c_3 x^p + c_4 x^{-p}, \tag{21}$$

where $p = \sqrt{\lambda + \frac{\kappa^2}{4\pi G}}$, with c_3 and c_4 arbitrary constants.

Thus the complete solution of equation (17) assumes the form

$$\psi(z, x) = [c_1 J_\nu(i\tilde{z}) + c_2 Y_\nu(i\tilde{z})] [c_3 x^p + c_4 x^{-p}]. \tag{22}$$

We thus have the general form of wave function in the back hole interior, expressed by

$$\Psi(\xi, \zeta, \phi) = \left[c_1 J_{\sqrt{\lambda}}(il_0 a\xi b\zeta) + c_2 Y_{\sqrt{\lambda}}(il_0 a\xi b\zeta) \right]$$

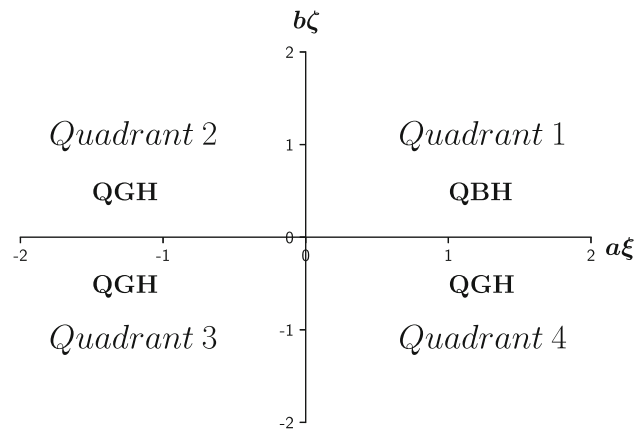


Fig. 1 Illustration of the four quadrants. Quantum black hole (QBH) solutions exist in Quadrant 1. Quantum grey hole (QGH) solutions exist in Quadrants 2, 3 and 4

$$\times \left[c_3 (a\xi)^{\sqrt{\lambda+k^2}} + c_4 (a\xi)^{-\sqrt{\lambda+k^2}} \right] e^{-i\kappa\phi}, \tag{23}$$

where $l_0 = \frac{r_0}{\hbar G}$ and $k^2 = \frac{\kappa^2}{4\pi G}$. Moreover, we note that if we had included a cosmological constant Λ , the constant κ^2 would be modified to $\kappa^2 + \Lambda$.

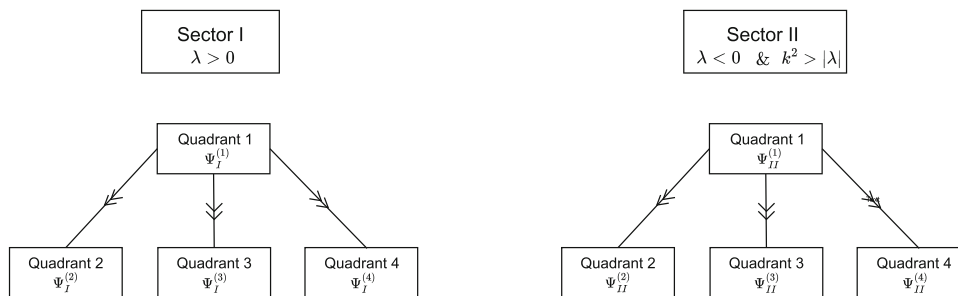
Depending on the relative magnitude of the eigenvalues, the Hilbert space splits into three nonoverlapping sectors, namely, Sectors I, II and III, with the first two sectors satisfying the DeWitt boundary condition, so that regular quantum black holes can exist in Sectors I and II.

Importantly, we see that the wave function explicitly depends on the parameters a and b . This property of the wave function plays a crucial role in our analysis. In particular, for $a = b = +1$, the wave function can be identified with quantum black hole (QBH) solutions. The other combinations of signs for a and b should correspond to other solutions that we call “quantum grey hole” (QGH) solutions. Figure 1 illustrates the QBH and QGH solutions in the four Quadrants.

Thus, there exist possibilities of transition from a quantum black hole to a quantum grey hole. This scenario translates into considering transitions from Quadrant 1 to the other Quadrants. Figure 2 illustrates QBH to QGH transitions in Sectors I and II, where regular QBHs exist.

At this point, it may be worth noting that Batic et al. [39,40] analyzed gravitational collapse employing the Wheeler–DeWitt equation in the Robertson–Walker minisuperspace representation and showed that the density of the collapsing dust is quantized without the appearance of a singularity. The difference in our results arises owing to the Kantowski–Sachs minisuperspace representation for the black hole interior with a Klein–Gordon field representing the zero-point vacuum fluctuations.

Fig. 2 Illustration of QBH to QGH transitions in Sectors I and II, where regular QBHs exist



5 Transition probability in Sector I

The black hole is said to belong to Sector I for the case $\lambda > 0$. In this Sector, the wave function satisfying the DeWitt boundary condition is obtained from (23) as

$$\Psi_I(\xi, \zeta, \phi) = C_2 J_{\sqrt{\lambda}}(il_0 a \xi b \zeta) (a \xi)^{-\sqrt{\lambda+k^2}} e^{-i\kappa \phi}. \tag{24}$$

Thus the wave function of the QBH in Quadrant 1 takes the form

$$\Psi_I^{(1)}(\xi, \zeta, \phi) = C_2 J_{\sqrt{\lambda}}(il_0 \xi \zeta) (\xi)^{-\sqrt{\lambda+k^2}} e^{-i\kappa \phi}. \tag{25}$$

On the other hand, the wave functions of the QGHs in Quadrants 2, 3 and 4 are respectively given by

$$\Psi_I^{(2)}(\xi, \zeta, \phi) = C_2 J_{\sqrt{\lambda}}(-il_0 \xi \zeta) (-\xi)^{-\sqrt{\lambda+k^2}} e^{-i\kappa \phi}, \tag{26}$$

$$\Psi_I^{(3)}(\xi, \zeta, \phi) = C_2 J_{\sqrt{\lambda}}(il_0 \xi \zeta) (-\xi)^{-\sqrt{\lambda+k^2}} e^{-i\kappa \phi}, \tag{27}$$

and

$$\Psi_I^{(4)}(\xi, \zeta, \phi) = C_2 J_{\sqrt{\lambda}}(-il_0 \xi \zeta) (\xi)^{-\sqrt{\lambda+k^2}} e^{-i\kappa \phi}. \tag{28}$$

The probability amplitude of black-to-grey hole transition from Quadrant 1 to Quadrant 2 is given by

$$\mathcal{A}_I^{1 \rightarrow 2} = \int d^3x \sqrt{h} \Psi_I^{(2)*} \Psi_I^{(1)} d\xi d\zeta. \tag{29}$$

Substituting for $\Psi_I^{(1)}$ and $\Psi_I^{(2)}$ from equations (25) and (26), we get

$$\begin{aligned} \mathcal{A}_I^{1 \rightarrow 2} &= C |C_2|^2 \int \xi \zeta^2 \left(J_{\sqrt{\lambda}}(-il_0 \xi \zeta) (-\xi)^{-\sqrt{\lambda+k^2}} \right)^* \\ &\quad \times J_{\sqrt{\lambda}}(il_0 \xi \zeta) (\xi)^{-\sqrt{\lambda+k^2}} d\xi d\zeta, \end{aligned} \tag{30}$$

where $C = 4\pi r_0 a b^2$.

The singularity is characterized by the limits $\xi \rightarrow \infty$, $\zeta \rightarrow 0$ and $\xi \zeta \rightarrow 0$. Consequently, we take the asymptotic form of the Bessel function $J_\nu(z)$ near $z \rightarrow 0$ with the

behavior [41,42]

$$J_\nu(z) \sim \frac{\left(\frac{1}{2}z\right)^\nu}{\Gamma(\nu+1)}. \tag{31}$$

With this asymptotic form, Eq. (30) reduces to

$$\begin{aligned} \mathcal{A}_I^{1 \rightarrow 2} &\sim C |C_2|^2 \left(\frac{\left(\frac{1}{2}il_0\right)^{\sqrt{\lambda}}}{\Gamma(\sqrt{\lambda}+1)} \right)^2 \left\{ (-1)^{-\sqrt{\lambda+k^2}} \right\}^* \\ &\quad \times \int \xi^{1+2\sqrt{\lambda}-2\sqrt{\lambda+k^2}} d\xi \int \zeta^{2+2\sqrt{\lambda}} d\zeta \end{aligned} \tag{32}$$

We carry out the integrations in (32) from the point of classical singularity to the fiducial length r_0 . Near the classical singularity $t \rightarrow 0$, $\xi \sim t^{-1/2}$ and $\zeta \sim t$. The first integral behaves as $\xi^{2+2\sqrt{\lambda}-2\sqrt{\lambda+k^2}} \sim t^{-1-1\sqrt{\lambda}+\sqrt{\lambda+k^2}}$, and the second integral looks like $\zeta^{3+2\sqrt{\lambda}} \sim t^{3+2\sqrt{\lambda}}$. Thus the overall behavior of (32) is $t^{2+\sqrt{\lambda}+\sqrt{\lambda+k^2}}$, that vanishes at the singularity, $t \rightarrow 0$, which corresponds to the lower limits of the integrals in (32). Since the contribution from the lower limits vanish, the integrals in (32) receive contributions from the upper limits, yielding the probability amplitude

$$\begin{aligned} \mathcal{A}_I^{1 \rightarrow 2} &\sim \frac{1}{2} C |C_2|^2 \left(\frac{\left(\frac{1}{2}il_0\right)^{\sqrt{\lambda}}}{\Gamma(\sqrt{\lambda}+1)} \right)^2 \left\{ (-1)^{-\sqrt{\lambda+k^2}} \right\}^* \\ &\quad \times \left(\frac{\left(\frac{r_0}{2GM}\right)^{\sqrt{\lambda+k^2}-1-\sqrt{\lambda}}}{1+\sqrt{\lambda}-\sqrt{\lambda+k^2}} \right) \left(\frac{r_0^{3+2\sqrt{\lambda}}}{3+2\sqrt{\lambda}} \right) \end{aligned} \tag{33}$$

Thus, for a quantum black hole in Sector I, the probability of black-to-grey hole transition from Quadrant 1 to Quadrant 2 is given by

$$\begin{aligned} \mathcal{P}_I^{1 \rightarrow 2} &= \left| \mathcal{A}_I^{1 \rightarrow 2} \right|^2 \sim \frac{1}{4} C^2 |C_2|^4 \left(\frac{\left(\frac{1}{2}il_0\right)^{\sqrt{\lambda}}}{\Gamma(\sqrt{\lambda}+1)} \right)^4 \\ &\quad \times \left(\frac{\left(\frac{r_0}{2GM}\right)^{\sqrt{\lambda+k^2}-1-\sqrt{\lambda}}}{1+\sqrt{\lambda}-\sqrt{\lambda+k^2}} \right)^2 \left(\frac{r_0^{3+2\sqrt{\lambda}}}{3+2\sqrt{\lambda}} \right)^2 \end{aligned} \tag{34}$$

Remaining within Sector I, we shall next calculate the transition probability for the black hole in Quadrant 1 transitioning into a grey hole in Quadrants 3 and 4. The corresponding probability amplitudes can be obtained from

$$\mathcal{A}_I^{1 \rightarrow 3} = \int d^3x \sqrt{h} \Psi_I^{(3)*} \Psi_I^{(1)} d\xi d\zeta \tag{35}$$

and

$$\mathcal{A}_I^{1 \rightarrow 4} = \int d^3x \sqrt{h} \Psi_I^{(4)*} \Psi_I^{(1)} d\xi d\zeta. \tag{36}$$

Substituting from (25), (27) and (28), and proceeding in a similar manner as before, these probability amplitudes are found to be

$$\begin{aligned} \mathcal{A}_I^{1 \rightarrow 3} \sim & \frac{1}{2} C |C_2|^2 \left(\frac{(\frac{1}{2} l_0)^{\sqrt{\lambda}}}{\Gamma(\sqrt{\lambda} + 1)} \right)^2 \left\{ (-1)^{-\sqrt{\lambda+k^2}} \right\}^* \\ & \times \left(\frac{(\frac{r_0}{2GM})^{\sqrt{\lambda+k^2}-1-\sqrt{\lambda}}}{1 + \sqrt{\lambda} - \sqrt{\lambda+k^2}} \right) \left(\frac{r_0^{3+2\sqrt{\lambda}}}{3 + 2\sqrt{\lambda}} \right) \end{aligned} \tag{37}$$

and

$$\begin{aligned} \mathcal{A}_I^{1 \rightarrow 4} \sim & \frac{1}{2} C |C_2|^2 \left(\frac{(\frac{1}{2} i l_0)^{\sqrt{\lambda}}}{\Gamma(\sqrt{\lambda} + 1)} \right)^2 \\ & \times \left(\frac{(\frac{r_0}{2GM})^{\sqrt{\lambda+k^2}-1-\sqrt{\lambda}}}{1 + \sqrt{\lambda} - \sqrt{\lambda+k^2}} \right) \left(\frac{r_0^{3+2\sqrt{\lambda}}}{3 + 2\sqrt{\lambda}} \right). \end{aligned} \tag{38}$$

It is noteworthy that these expressions for $\mathcal{A}_I^{1 \rightarrow 3}$ and $\mathcal{A}_I^{1 \rightarrow 4}$ in (37), and (38) differ from $\mathcal{A}_I^{1 \rightarrow 2}$ given by (33) only in the phase.

Consequently, the corresponding probabilities, namely, $\mathcal{P}_I^{1 \rightarrow 3} = |\mathcal{A}_I^{1 \rightarrow 3}|^2$ and $\mathcal{P}_I^{1 \rightarrow 4} = |\mathcal{A}_I^{1 \rightarrow 4}|^2$, are both equal to $\mathcal{P}_I^{1 \rightarrow 2} = |\mathcal{A}_I^{1 \rightarrow 2}|^2$, so that

$$\mathcal{P}_I^{1 \rightarrow 2} = \mathcal{P}_I^{1 \rightarrow 3} = \mathcal{P}_I^{1 \rightarrow 4}. \tag{39}$$

We may thus conclude that a quantum black hole in Sector I has equal probability to make transition to any of the quantum grey hole states in Quadrants 2, 3 or 4 in the deep quantum regime.

Figures 3, 5 and 4 illustrate this probability of transition (denoted by \mathcal{P}_I) with respect to the eigenvalues λ and κ in various perspectives. It is clear from these figures that there exist continuous resonance trajectories in the (λ, k) plane where the black-to-grey hole transition is highly favoured in the deep quantum regime.

It may be worth noting that the above features remain unaltered with respect to a general operator ordering, $(\xi \hat{P}_\xi)^2 \rightarrow$

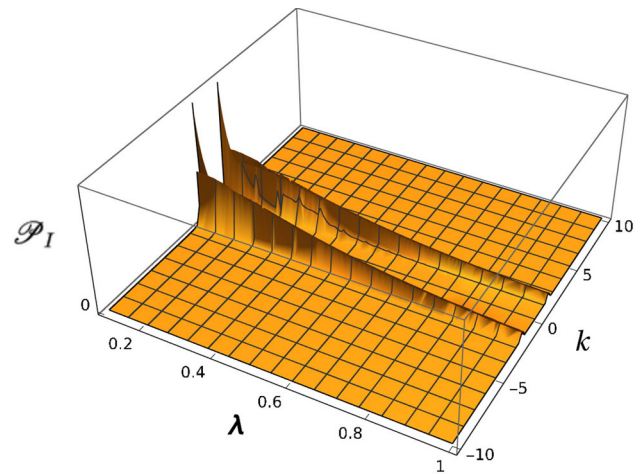


Fig. 3 Probability of black-to-grey hole transition with respect to the eigenvalues (λ, k) for a quantum black hole in Sector I

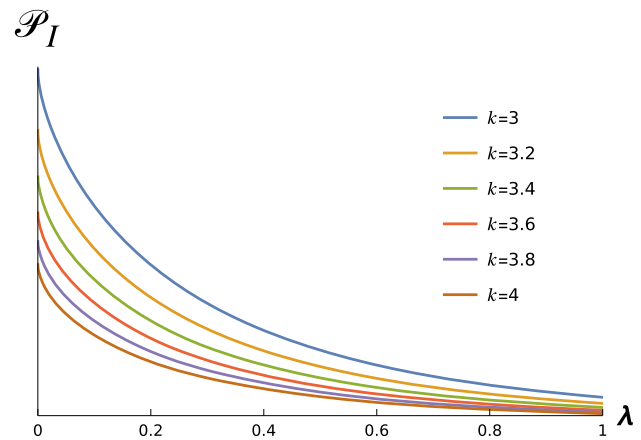


Fig. 4 Probability of black-to-grey hole transition with respect to the eigenvalue λ at $k = 3.0, 3.2, 3.4, 3.6, 3.8$ and 4.0 for a quantum black hole in Sector I

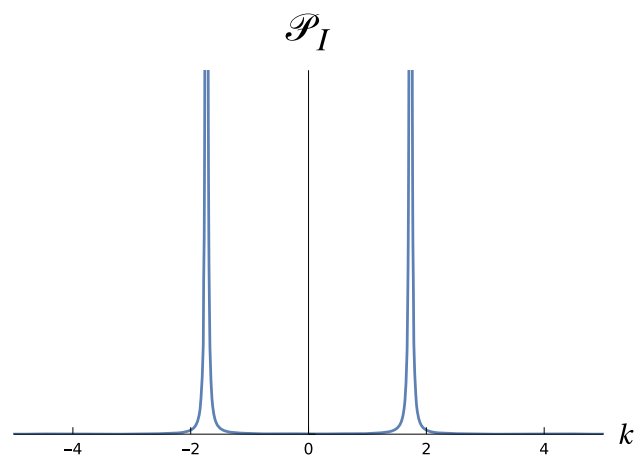


Fig. 5 Probability of black-to-grey hole transition with respect to the eigenvalue k at $\lambda = 1$ for a quantum black hole in Sector I

$\xi^{2-n} \hat{P}_\xi \xi^n \hat{P}_\xi$, in the Hamiltonian (13), where n is the ordering parameter. This changes the third term in the Wheeler–DeWitt equation (14), so that $\frac{\xi}{2} \frac{\partial}{\partial \xi} \rightarrow n \frac{\xi}{2} \frac{\partial}{\partial \xi}$. Consequently, the second terms in Eqs. (18) and (19) are modified as $z \frac{\partial Z}{\partial z} \rightarrow (2-n)z \frac{\partial Z}{\partial z}$ and $x \frac{\partial X}{\partial x} \rightarrow nx \frac{\partial X}{\partial x}$.

Hence the expression (34) for the transition probability has the same form with the modifications $\lambda \rightarrow \lambda' = \lambda - \frac{1}{4}(n-1)^2$ together with $\frac{r_0^{3+2\sqrt{\lambda}}}{3+2\sqrt{\lambda}} \rightarrow \frac{r_0^{3+2\sqrt{\lambda'}+(n-1)}}{3+2\sqrt{\lambda'}+(n-1)}$. The three transition probabilities still maintain the equality (39).

6 Transition probability in Sector II

The black hole is said to belong to Sector II for the case when $\lambda < 0$ and $k^2 > |\lambda|$. In this Sector, the wave function satisfying the DeWitt boundary condition is obtained from (23) as

$$\Psi_{II}(\xi, \zeta, \phi) = [C_2 J_{i\eta}(il_0 a \xi b \zeta) + C_4 Y_{i\eta}(il_0 a \xi b \zeta)] \times (a \xi)^{-\sqrt{k^2-\eta^2}} e^{-i\kappa\phi}, \tag{40}$$

where $\lambda = -\eta^2$, with η real.

Thus in Quadrant 1, where $a = b = +1$, the wave function of the QBH takes the form

$$\Psi_{II}^{(1)}(\xi, \zeta, \phi) = [C_2 J_{i\eta}(il_0 \xi \zeta) + C_4 Y_{i\eta}(il_0 \xi \zeta)] \times \xi^{-\sqrt{k^2-\eta^2}} e^{-i\kappa\phi}. \tag{41}$$

In Quadrants 2, 3 and 4, in contrast, the wave functions of the QGHs take the forms

$$\Psi_{II}^{(2)}(\xi, \zeta, \phi) = [C_2 J_{i\eta}(-il_0 \xi \zeta) + C_4 Y_{i\eta}(-il_0 \xi \zeta)] \times (-\xi)^{-\sqrt{k^2-\eta^2}} e^{-i\kappa\phi}, \tag{42}$$

$$\Psi_{II}^{(3)}(\xi, \zeta, \phi) = [C_2 J_{i\eta}(il_0 \xi \zeta) + C_4 Y_{i\eta}(il_0 \xi \zeta)] \times (-\xi)^{-\sqrt{k^2-\eta^2}} e^{-i\kappa\phi} \tag{43}$$

and

$$\Psi_{II}^{(4)}(\xi, \zeta, \phi) = [C_2 J_{i\eta}(-il_0 \xi \zeta) + C_4 Y_{i\eta}(-il_0 \xi \zeta)] \times \xi^{-\sqrt{k^2-\eta^2}} e^{-i\kappa\phi}. \tag{44}$$

In this Sector, the transition amplitude of black-to-grey hole metamorphosis from quadrant 1 to 2 obtained from

$$\mathcal{A}_{II}^{1 \rightarrow 2} = \int d^3x \sqrt{h} \Psi_{II}^{(2)*} \Psi_{II}^{(1)} d\xi d\zeta. \tag{45}$$

Substituting the wave functions $\Psi_{II}^{(1)}$ and $\Psi_{II}^{(2)}$ from equations (41) and (42), we get

$$\mathcal{A}_{II}^{1 \rightarrow 2} = C \left(|C_2|^2 \mathcal{I}_1 + C_2^* C_4 \mathcal{I}_2 + C_4^* C_2 \mathcal{I}_3 + |C_4|^2 \mathcal{I}_4 \right), \tag{46}$$

where $C = 4\pi r_0 a b^2$, and

$$\mathcal{I}_1 = \int \xi \zeta^2 \left\{ J_{i\eta}(-il_0 \xi \zeta) (-\xi)^{-\sqrt{k^2-\eta^2}} \right\}^* \times J_{i\eta}(il_0 \xi \zeta) (\xi)^{-\sqrt{k^2-\eta^2}} d\xi d\zeta, \tag{47}$$

$$\mathcal{I}_2 = \int \xi \zeta^2 \left\{ J_{i\eta}(-il_0 \xi \zeta) (-\xi)^{-\sqrt{k^2-\eta^2}} \right\}^* \times Y_{i\eta}(il_0 \xi \zeta) (\xi)^{-\sqrt{k^2-\eta^2}} d\xi d\zeta, \tag{48}$$

$$\mathcal{I}_3 = \int \xi \zeta^2 \left\{ Y_{i\eta}(-il_0 \xi \zeta) (-\xi)^{-\sqrt{k^2-\eta^2}} \right\}^* \times J_{i\eta}(il_0 \xi \zeta) (\xi)^{-\sqrt{k^2-\eta^2}} d\xi d\zeta, \tag{49}$$

and

$$\mathcal{I}_4 = \int \xi \zeta^2 \left\{ Y_{i\eta}(-il_0 \xi \zeta) (-\xi)^{-\sqrt{k^2-\eta^2}} \right\}^* \times Y_{i\eta}(il_0 \xi \zeta) (\xi)^{-\sqrt{k^2-\eta^2}} d\xi d\zeta. \tag{50}$$

Since the singularity is characterized by the limits $\xi \rightarrow \infty$, $\zeta \rightarrow 0$ and $\xi \zeta \rightarrow 0$, we take the asymptotic forms of the Bessel functions $J_\nu(z)$ and $Y_\nu(z)$, having behaviors [41, 42] near $z \rightarrow 0$ as

$$J_\nu(z) \sim \frac{\left(\frac{1}{2}z\right)^\nu}{\Gamma(\nu+1)} \tag{51}$$

and

$$Y_\nu(z) \sim -\frac{1}{\pi} \frac{\Gamma(\nu)}{\left(\frac{1}{2}z\right)^\nu}. \tag{52}$$

In these limits, the integrals (47)–(49) and (50) have the asymptotic forms

$$\mathcal{I}_1 \sim \left\{ (-1)^{-\sqrt{k^2-\eta^2}} \right\}^* \frac{\sinh \pi \eta}{\pi \eta} \times \int \xi^{1-2\sqrt{k^2-\eta^2}} d\xi \int \zeta^2 d\zeta, \tag{53}$$

$$\mathcal{I}_2 \sim -\left\{ (-1)^{-\sqrt{k^2-\eta^2}} \right\}^* \frac{\Gamma(i\eta)}{\pi \Gamma(-i\eta+1)} \left(\frac{1}{2}il_0\right)^{-2i\eta} \times \int \xi^{1-2i\eta-2\sqrt{k^2-\eta^2}} d\xi \int \zeta^{2-2i\eta} d\zeta, \tag{54}$$

$$\mathcal{I}_3 \sim - \left\{ (-1)^{-\sqrt{k^2-\eta^2}} \right\}^* \frac{\Gamma(-i\eta)}{\pi\Gamma(i\eta+1)} \left(\frac{1}{2} il_0 \right)^{2i\eta} \times \int \xi^{1+2i\eta-2\sqrt{k^2-\eta^2}} d\xi \int \zeta^{2+2i\eta} d\zeta, \tag{55}$$

and

$$\mathcal{I}_4 \sim \left\{ (-1)^{-\sqrt{k^2-\eta^2}} \right\}^* \frac{1}{\pi\eta \sinh \pi\eta} \times \int \xi^{1-2\sqrt{k^2-\eta^2}} d\xi \int \zeta^2 d\zeta. \tag{56}$$

We carry out the integrations in (53)–(56) from the classical singularity to the fiducial radius r_0 . We note that $\xi \sim t^{-1/2}$ and $\zeta \sim t$ near the classical singularity $t \rightarrow 0$. Consequently, the first integrals in each of the above equations behave like $\xi^{2-2\sqrt{k^2-\eta^2}} \sim t^{-1+\sqrt{k^2-\eta^2}}$, and the second integrals like $\zeta^3 \sim t^3$. Thus, all these integrals have an overall behavior of $t^{2+\sqrt{k^2-\eta^2}}$, which vanishes at the singularity, $t \rightarrow 0$. This behavior at the lower limits remains valid for the integrals in (55) and (56) where the magnitude of the oscillating factor $t^{\pm i\eta} = e^{\pm i\eta \ln t}$ remains bounded within unity. With vanishing contribution from the lower limits, the integrals in (53)–(56) yield non-zero contributions only from the upper limits, leading to

$$\mathcal{I}_1 \sim \left\{ (-1)^{-\sqrt{k^2-\eta^2}} \right\}^* \frac{\sinh \pi\eta}{\pi\eta} \times \left(\frac{\left(\frac{r_0}{2GM}\right)\sqrt{k^2-\eta^2-1}}{2-2\sqrt{k^2-\eta^2}} \right) \left(\frac{r_0^3}{3} \right), \tag{57}$$

$$\mathcal{I}_2 \sim - \left\{ (-1)^{-\sqrt{k^2-\eta^2}} \right\}^* \frac{\Gamma(i\eta)}{\pi\Gamma(-i\eta+1)} \left(\frac{1}{2} il_0 \right)^{-2i\eta} \times \left(\frac{\left(\frac{r_0}{2GM}\right)\sqrt{k^2-\eta^2+i\eta-1}}{2-2i\eta-2\sqrt{k^2-\eta^2}} \right) \left(\frac{r_0^{3-2i\eta}}{3-2i\eta} \right), \tag{58}$$

$$\mathcal{I}_3 \sim - \left\{ (-1)^{-\sqrt{k^2-\eta^2}} \right\}^* \frac{\Gamma(-i\eta)}{\pi\Gamma(i\eta+1)} \left(\frac{1}{2} il_0 \right)^{2i\eta} \times \left(\frac{\left(\frac{r_0}{2GM}\right)\sqrt{k^2-\eta^2-i\eta-1}}{2+2i\eta-2\sqrt{k^2-\eta^2}} \right) \left(\frac{r_0^{3+2i\eta}}{3+2i\eta} \right), \tag{59}$$

and

$$\mathcal{I}_4 \sim \left\{ (-1)^{-\sqrt{k^2-\eta^2}} \right\}^* \frac{1}{\pi\eta \sinh \pi\eta} \times \left(\frac{\left(\frac{r_0}{2GM}\right)\sqrt{k^2-\eta^2-1}}{2-2\sqrt{k^2-\eta^2}} \right) \left(\frac{r_0^3}{3} \right). \tag{60}$$

Employing these expressions from (57)–(60), the probability amplitude given by (46) is found to be

$$\mathcal{A}_{II}^{1 \rightarrow 2} \sim C \left\{ (-1)^{-\sqrt{k^2-\eta^2}} \right\}^* \left[\left\{ |C_2|^2 \sinh \pi\eta + \frac{|C_4|^2}{\sinh \pi\eta} \right\} \times \left\{ \frac{1}{\pi\eta} \left(\frac{\left(\frac{r_0}{2GM}\right)\sqrt{k^2-\eta^2-1}}{2-2\sqrt{k^2-\eta^2}} \right) \left(\frac{r_0^3}{3} \right) \right\} - 2\text{Re} \left\{ C_4^* C_2 \frac{\Gamma(-i\eta)}{\pi\Gamma(i\eta+1)} \left(\frac{1}{2} il_0 \right)^{2i\eta} \times \left(\frac{\left(\frac{r_0}{2GM}\right)\sqrt{k^2-\eta^2-i\eta-1}}{2+2i\eta-2\sqrt{k^2-\eta^2}} \right) \left(\frac{r_0^{3+2i\eta}}{3+2i\eta} \right) \right\} \right]. \tag{61}$$

Thus, for a quantum black hole in Sector II, the probability of black-to-grey hole transition from Quadrant 1 to Quadrant 2 is given by

$$\mathcal{P}_{II}^{1 \rightarrow 2} = |\mathcal{A}_{II}^{1 \rightarrow 2}|^2 \sim C^2 \left[\left\{ |C_2|^2 \sinh \pi\eta + \frac{|C_4|^2}{\sinh \pi\eta} \right\} \times \left\{ \frac{1}{\pi\eta} \left(\frac{\left(\frac{r_0}{2GM}\right)\sqrt{k^2-\eta^2-1}}{2-2\sqrt{k^2-\eta^2}} \right) \left(\frac{r_0^3}{3} \right) \right\} - 2\text{Re} \left\{ C_4^* C_2 \frac{\Gamma(-i\eta)}{\pi\Gamma(i\eta+1)} \left(\frac{1}{2} il_0 \right)^{2i\eta} \times \left(\frac{\left(\frac{r_0}{2GM}\right)\sqrt{k^2-\eta^2-i\eta-1}}{2+2i\eta-2\sqrt{k^2-\eta^2}} \right) \left(\frac{r_0^{3+2i\eta}}{3+2i\eta} \right) \right\} \right]^2. \tag{62}$$

Remaining within Sector II, we shall next calculate the transition probability for the black hole in Quadrant 1 transitioning into a grey hole in Quadrants 3 and 4. The corresponding probability amplitudes can be obtained from

$$\mathcal{A}_{II}^{1 \rightarrow 3} = \int d^3x \sqrt{h} \Psi_{II}^{(3)*} \Psi_{II}^{(1)} d\xi d\zeta \tag{63}$$

and

$$\mathcal{A}_{II}^{1 \rightarrow 4} = \int d^3x \sqrt{h} \Psi_{II}^{(4)*} \Psi_{II}^{(1)} d\xi d\zeta \tag{64}$$

Substituting from (41), (43) and (44), and proceeding in a similar manner as before, these probability amplitudes are found to be

$$\begin{aligned}
 \mathcal{A}_{II}^{1 \rightarrow 3} &\sim C \left\{ (-1)^{-\sqrt{k^2 - \eta^2}} \right\}^* \left[\left\{ |C_2|^2 \sinh \pi \eta + \frac{|C_4|^2}{\sinh \pi \eta} \right\} \right. \\
 &\times \left. \left\{ \frac{1}{\pi \eta} \left(\frac{r_0}{2GM} \right)^{\sqrt{k^2 - \eta^2} - 1} \left(\frac{r_0^3}{3} \right) \right\} \right. \\
 &- 2 \operatorname{Re} \left\{ C_4^* C_2 \frac{\Gamma(-i\eta)}{\pi \Gamma(i\eta + 1)} \left(\frac{1}{4} l_0^2 \right)^{i\eta} \right. \\
 &\times \left. \left. \left(\frac{r_0}{2GM} \right)^{\sqrt{k^2 - \eta^2} - i\eta - 1} \left(\frac{r_0^{3+2i\eta}}{3 + 2i\eta} \right) \right\} \right] \quad (65)
 \end{aligned}$$

and

$$\begin{aligned}
 \mathcal{A}_{II}^{1 \rightarrow 4} &\sim C \left\{ (-1)^{-\sqrt{k^2 - \eta^2}} \right\}^* \left[\left\{ |C_2|^2 \sinh \pi \eta + \frac{|C_4|^2}{\sinh \pi \eta} \right\} \right. \\
 &\times \left. \left\{ \frac{1}{\pi \eta} \left(\frac{r_0}{2GM} \right)^{\sqrt{k^2 - \eta^2} - 1} \left(\frac{r_0^3}{3} \right) \right\} \right. \\
 &- 2 \operatorname{Re} \left\{ C_4^* C_2 \frac{\Gamma(-i\eta)}{\pi \Gamma(i\eta + 1)} \left(\frac{1}{2} i l_0 \right)^{2i\eta} \right. \\
 &\times \left. \left. \left(\frac{r_0}{2GM} \right)^{\sqrt{k^2 - \eta^2} - i\eta - 1} \left(\frac{r_0^{3+2i\eta}}{3 + 2i\eta} \right) \right\} \right] \quad (66)
 \end{aligned}$$

It is noteworthy that these expressions for $\mathcal{A}_{II}^{1 \rightarrow 3}$ and $\mathcal{A}_{II}^{1 \rightarrow 4}$ in (65), and (66) differ from $\mathcal{A}_{II}^{1 \rightarrow 2}$ given by (61) only in the phase.

Consequently, the corresponding probabilities, namely, $\mathcal{P}_{II}^{1 \rightarrow 3} = |\mathcal{A}_{II}^{1 \rightarrow 3}|^2$ and $\mathcal{P}_{II}^{1 \rightarrow 4} = |\mathcal{A}_{II}^{1 \rightarrow 4}|^2$, are both equal to $\mathcal{P}_{II}^{1 \rightarrow 2} = |\mathcal{A}_{II}^{1 \rightarrow 2}|^2$, so that

$$\mathcal{P}_{II}^{1 \rightarrow 2} = \mathcal{P}_{II}^{1 \rightarrow 3} = \mathcal{P}_{II}^{1 \rightarrow 4}. \quad (67)$$

We may thus conclude that a quantum black hole in Sector II has equal probability to make transition to any of the quantum grey hole states in Quadrants 2, 3 or 4 in the deep quantum regime.

Figures 6, 7 and 8 illustrate this probability of transition (denoted by \mathcal{P}_{II}) with respect to the eigenvalues λ and κ in various perspectives. It is clear from these figures that there exist continuous resonance trajectories in the (λ, κ) plane where the black-to-grey hole transition is highly favoured in the deep quantum regime.

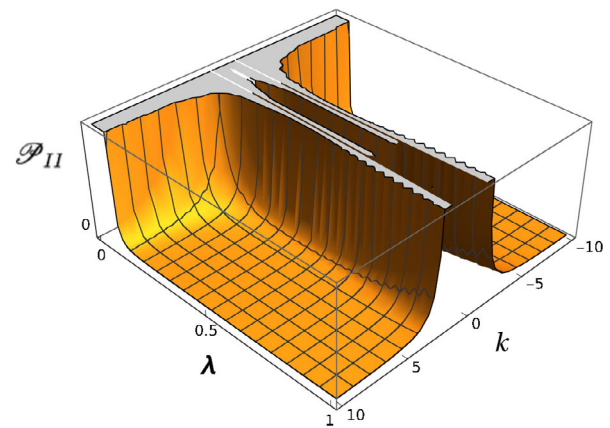


Fig. 6 Probability of black-to-grey hole transition with respect to the eigenvalues (λ, κ) for a quantum black hole in Sector II

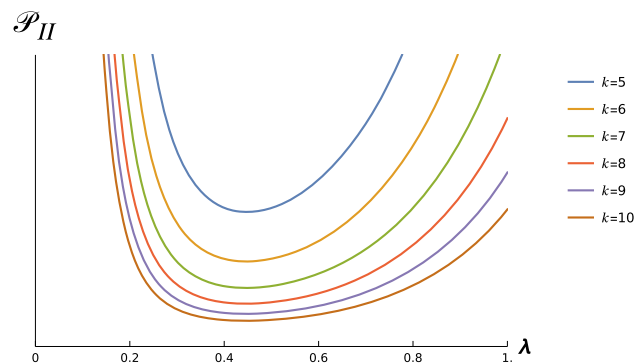


Fig. 7 Probability of black-to-grey hole transition with respect to the eigenvalue λ at $\kappa = 5, 6, 7, 8, 9$ and 10 for a quantum black hole in Sector II

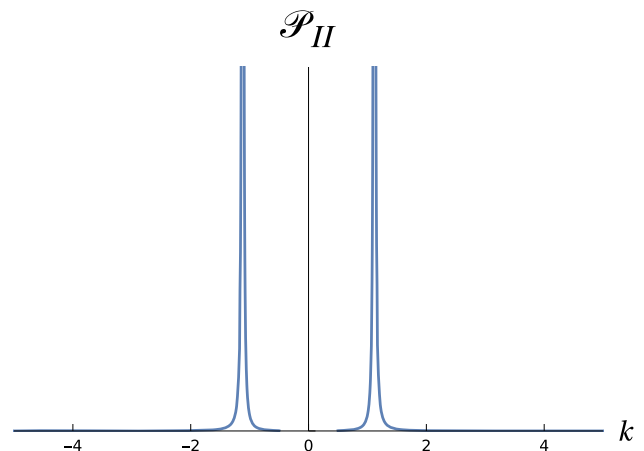


Fig. 8 Probability of black-to-grey hole transition with respect to the eigenvalue κ at $\lambda = 0.5$ for a quantum black hole in Sector II

We once again find that the above features remain unaltered with respect to a general operator ordering as stated earlier in the case of Sector I. Now the expression (62) for the transition probability has the same form with the modifica-

tions $\eta^2 \rightarrow \eta'^2 = \eta^2 - \frac{1}{4}(n-1)^2$ together with $\frac{r_0^3}{3} \rightarrow \frac{r_0^{3+(n-1)}}{3+(n-1)}$ and $\frac{r_0^{3+2i\eta}}{3+2i\eta} \rightarrow \frac{r_0^{3+2i\eta'+(n-1)}}{3+2i\eta'+(n-1)}$. The three transition probabilities still maintain the equality (67).

7 Discussion and conclusion

Upon appreciating the importance of the deep quantum regime of a black hole in undergoing any kind of transition to other quantum states, we considered in this paper the quantum gravitational wave function of the black hole interior spacetime. In order to investigate into this scenario, we first modelled the black hole interior with a Kantowski–Sachs metric containing parameters (a, b) that play a crucial role in determining the wave function of the interior spacetime (although these parameters have no role to play classically). Additionally, we included a Klein–Gordon field in order to account for inevitable zero-point quantum vacuum fluctuations in its simplest form.

With this pedestal, we solved the Wheeler–DeWitt equation and obtained a general solution giving the black hole interior wave function that depends on the parameters (a, b) . Resolution of the classical singularity with the DeWitt boundary condition occurs in two sectors of the Hilbert space having distinct relative magnitudes of the eigenvalues (λ, κ) . In these two sectors (Sectors I and II), regular quantum black holes can exist.

It is important to note that the metric (1) is exactly equivalent to $ds^2 = -\alpha^2(t)dt^2 + \xi^2(t)dr^2 + \zeta^2(t)d\Omega^2$ in the classical sense. However, quantum mechanically, the sign parameters a and b make a substantial difference in the quantum mechanical picture since they appear in the expression of the interior wave function, which depends on the square root of the spatial metric coefficients.

Owing to the presence of the model parameters (a, b) in the wave function, the solutions have distinct quantum mechanical characters in the four quadrants of the ab -plane. The wave function in the first quadrant for $a = b = +1$ represents the normal solution for regular quantum black holes. On the other hand, the wave functions in the second, third and fourth quadrants, with other signs of the parameters a and b , have quite different quantum mechanical nature from that in the first quadrant, and they are called herein regular quantum grey holes. Consequently, a regular quantum black hole in the first quadrant can make a transition to a regular quantum grey hole in the second, third or fourth quadrant, as illustrated in Fig. 2.

We calculated the probability of such transitions for a quantum black hole existing in each of the Sectors I and II. We found that probability of such transitions are equal in a given Sector [Eqs. (39) and (67)], and quantum black

holes existing in different Sectors have different transition probabilities ($\mathcal{P}_I \neq \mathcal{P}_{II}$).

Interestingly, the transition probabilities (\mathcal{P}_I and \mathcal{P}_{II}) exhibit resonances in the eigenvalue plane (λ, k) where the black-to-grey hole transition is highly favored, as shown in Figs. 3 and 6. These resonances are clearer in Figs. 5 and 8 that exhibit the profiles on a constant- λ plane.

It is therefore clear from our analysis that the quantum black hole can make a transition to any of the grey hole states before transitioning to a bouncing white hole scenario. In fact, such intermediate states have been already speculated in the work of Volovik [43]. The quantum grey hole states can be identified with such intermediate states.

Thus, our simple consideration with a Kantowski–Sachs metric for the black hole interior permeated with zero-point vacuum fluctuations of a Klein–Gordon field reveals the existence of not only regular quantum black holes but also the existence of other kinds of solutions that we call regular quantum grey holes. The existence of new solutions gives rise to the novel possibility of a quantum black hole making a transition to a quantum grey hole. Such a transition process should play a crucial role towards the end of black hole evaporation.

Acknowledgements The authors are grateful to Prof. Abhay Ashtekar for bringing some of his papers into their attention. They are also grateful to Prof. Steven Carlip for many useful discussions in the context of Wheeler–DeWitt equation. Harpreet Singh is supported by the Prime Minister’s Research Fellowship (PMRF), Ministry of Education, Government of India.

Data Availability Statement This manuscript has no associated data. [Author’s comment: Data sharing not applicable to this article as no datasets were generated or analysed during the current study].

Code Availability Statement This manuscript has no associated code/software. [Author’s comment: Code/Software sharing not applicable to this article as no code/software was generated or analysed during the current study].

Open Access This article is licensed under a Creative Commons Attribution 4.0 International License, which permits use, sharing, adaptation, distribution and reproduction in any medium or format, as long as you give appropriate credit to the original author(s) and the source, provide a link to the Creative Commons licence, and indicate if changes were made. The images or other third party material in this article are included in the article’s Creative Commons licence, unless indicated otherwise in a credit line to the material. If material is not included in the article’s Creative Commons licence and your intended use is not permitted by statutory regulation or exceeds the permitted use, you will need to obtain permission directly from the copyright holder. To view a copy of this licence, visit <http://creativecommons.org/licenses/by/4.0/>.
Funded by SCOAP³.

References

1. S.W. Hawking, Black hole explosions? *Nature* **248**(5443), 30–31 (1974)

2. S.W. Hawking, Particle creation by black holes. *Commun. Math. Phys.* **43**(3), 199–220 (1975). <https://doi.org/10.1007/BF02345020>
3. R. Penrose, Gravitational collapse and space-time singularities. *Phys. Rev. Lett.* **14**, 57–59 (1965). <https://doi.org/10.1103/PhysRevLett.14.57>
4. S.W. Hawking, Singularities in the universe. *Phys. Rev. Lett.* **17**, 444–445 (1966). <https://doi.org/10.1103/PhysRevLett.17.444>
5. S.W. Hawking, R. Penrose, The singularities of gravitational collapse and cosmology. *Proc. R. Soc. Lond. A* **314**(1519), 529–548 (1970)
6. S.W. Hawking, Black holes in general relativity. *Commun. Math. Phys.* **25**, 152–166 (1972)
7. S.W. Hawking, Breakdown of predictability in gravitational collapse. *Phys. Rev. D* **14**, 2460–2473 (1976). <https://doi.org/10.1103/PhysRevD.14.2460>
8. J. Bardeen, Non-singular general relativistic gravitational collapse, in *Proceedings of the 5th International Conference on Gravitation and the Theory of Relativity* (Publishing House of Tbilisi University, Georgia, 1968), p. 87.
9. S.A. Hayward, Formation and evaporation of nonsingular black holes. *Phys. Rev. Lett.* **96**, 031103 (2006). <https://doi.org/10.1103/PhysRevLett.96.031103>
10. S.A. Hayward, The disinformation problem for black holes (conference version) (2005). [arXiv:gr-qc/0504037](https://arxiv.org/abs/gr-qc/0504037)
11. M.B. Green, J.H. Schwarz, E. Witten, *Superstring Theory*, vol. 1, 2 (Cambridge University Press, Cambridge, 2012)
12. J. Polchinski, *String Theory*, vol. 1, 2 (Cambridge University Press, Cambridge, 1998)
13. A. Ashtekar, C. Rovelli, L. Smolin, Weaving a classical metric with quantum threads. *Phys. Rev. Lett.* **69**, 237–240 (1992). <https://doi.org/10.1103/PhysRevLett.69.237>
14. C. Rovelli, L. Smolin, Loop space representation of quantum general relativity. *Nucl. Phys. B* **331**(1), 80–152 (1990)
15. C. Rovelli, *Quantum Gravity* (Cambridge University Press, Cambridge, 2004)
16. B.R. Greene, D.R. Morrison, A. Strominger, Black hole condensation and the unification of string vacua. *Nucl. Phys. B* **451**(1–2), 109–120 (1995)
17. E. Witten, String theory and black holes. *Phys. Rev. D* **44**, 314–324 (1991). <https://doi.org/10.1103/PhysRevD.44.314>
18. G.T. Horowitz, S.F. Ross, Possible resolution of black hole singularities from large n gauge theory. *J. High Energy Phys.* **1998**(04), 015 (1998). <https://doi.org/10.1088/1126-6708/1998/04/015>
19. G. Gibbons, G.T. Horowitz, P. Townsend, Higher-dimensional resolution of dilatonic black-hole singularities. *Class. Quantum Gravity* **12**(2), 297 (1995)
20. L. Modesto, Disappearance of the black hole singularity in loop quantum gravity. *Phys. Rev. D* **70**, 124009 (2004). <https://doi.org/10.1103/PhysRevD.70.124009>
21. R. Gambini, J. Pullin, Black holes in loop quantum gravity: the complete space-time. *Phys. Rev. Lett.* **101**, 161301 (2008). <https://doi.org/10.1103/PhysRevLett.101.161301>
22. L. Smolin, *The Life of the Cosmos* (Oxford University Press, New York, 1997)
23. V.P. Frolov, G.A. Vilkovisky, Spherically symmetric collapse in quantum gravity. *Phys. Lett. B* **106**(4), 307–313 (1981). [https://doi.org/10.1016/0370-2693\(81\)90542-6](https://doi.org/10.1016/0370-2693(81)90542-6)
24. P. Hájek, J. Kijowski, Covariant gauge fixing and Kuchař decomposition. *Phys. Rev. D* **61**, 024037 (1999). <https://doi.org/10.1103/PhysRevD.61.024037>
25. P. Hájek, C. Kiefer, Singularity avoidance by collapsing shells in quantum gravity. *Int. J. Mod. Phys. D* **10**(06), 775–779 (2001). <https://doi.org/10.1142/S0218271801001578>
26. P. Hájek, C. Kiefer, Embedding variables in the canonical theory of gravitating shells. *Nucl. Phys. B* **603**(3), 531–554 (2001). [https://doi.org/10.1016/S0550-3213\(01\)00141-9](https://doi.org/10.1016/S0550-3213(01)00141-9)
27. M. Ambrus, P. Hájek, Quantum superposition principle and gravitational collapse: scattering times for spherical shells. *Phys. Rev. D* **72**, 064025 (2005). <https://doi.org/10.1103/PhysRevD.72.064025>
28. A. Ashtekar, T. Pawłowski, P. Singh, Quantum nature of the big bang. *Phys. Rev. Lett.* **96**, 141301 (2006). <https://doi.org/10.1103/PhysRevLett.96.141301>
29. A. Ashtekar, T. Pawłowski, P. Singh, K. Vandersloot, Loop quantum cosmology of $k = 1$ FRW models. *Phys. Rev. D* **75**, 024035 (2007). <https://doi.org/10.1103/PhysRevD.75.024035>
30. H.M. Haggard, C. Rovelli, Quantum-gravity effects outside the horizon spark black to white hole tunneling. *Phys. Rev. D* **92**, 104020 (2015). <https://doi.org/10.1103/PhysRevD.92.104020>
31. T. De Lorenzo, A. Perez, Improved black hole fireworks: asymmetric black-hole-to-white-hole tunneling scenario. *Phys. Rev. D* **93**, 124018 (2016). <https://doi.org/10.1103/PhysRevD.93.124018>
32. M. Han, C. Rovelli, F. Soltani, Geometry of the black-to-white hole transition within a single asymptotic region. *Phys. Rev. D* **107**, 064011 (2023). <https://doi.org/10.1103/PhysRevD.107.064011>
33. A. Rignon-Bret, C. Rovelli, Black to white transition of a charged black hole. *Phys. Rev. D* **105**, 086003 (2022). <https://doi.org/10.1103/PhysRevD.105.086003>
34. P. Frisoni, Numerical approach to the black-to-white hole transition. *Phys. Rev. D* **107**, 126012 (2023). <https://doi.org/10.1103/PhysRevD.107.126012>
35. J.A. Wheeler, *Relativity Groups and Topology, 1963 Les Houches Lectures* (Gordon and Breach Science Publishers Inc, New York, 1964)
36. B.S. DeWitt, Quantum theory of gravity. I. The canonical theory. *Phys. Rev.* **160**, 1113–1148 (1967). <https://doi.org/10.1103/PhysRev.160.1113>
37. R. Kantowski, R.K. Sachs, Some spatially homogeneous anisotropic relativistic cosmological models. *J. Math. Phys.* **7**(3), 443–446 (1966)
38. H. Singh, M.K. Nandy, Quantum nature of spacetime near the black hole singularity. *Eur. Phys. J. C* **84**(7), 700 (2024). <https://doi.org/10.1140/epjc/s10052-024-13041-9>
39. D. Batic, M. Nowakowski, Gravitational collapse via Wheeler–Dewitt equation. *Ann. Phys.* **461**, 169579 (2024). <https://doi.org/10.1016/j.aop.2023.169579>
40. D. Batic, M. Nowakowski, N.G. Kelkar, Wheeler–Dewitt equation and the late gravitational collapse: effects of factor ordering and the tunneling scenario. *Ann. Phys.* **469**, 169773 (2024). <https://doi.org/10.1016/j.aop.2024.169773>
41. M. Abramowitz, I.A. Stegun, *Handbook of Mathematical Functions with Formulas, Graphs, and Mathematical Tables*, vol. 55 (United States Department of Commerce, National Bureau of Standards, New York, 1948)
42. I.S. Gradshteyn, I.M. Ryzhik, *Table of Integrals, Series, and Products* (Academic Press, New York, 2014)
43. G.E. Volovik, From black hole to white hole via the intermediate static state. *Mod. Phys. Lett. A* **36**(17), 2150117 (2021). <https://doi.org/10.1142/S0217732321501170>